PNAS
www.pnas.org

Supplementary Information for

Tissue-specific contributions of Tmem79 to atopic dermatitis and mast cell-mediated histaminergic itch

Joshua J. Emrick, Anubhav Mathur, Jessica Wei, Elena O. Gracheva, Karsten Gronert, Michael D. Rosenblum, and David Julius

Corresponding author: David Julius
Email: David.Julius@ucsf.edu

This PDF file includes:

Figs. S1 to S8

www.pnas.org/cgi/doi/10.1073/pnas.1814132115

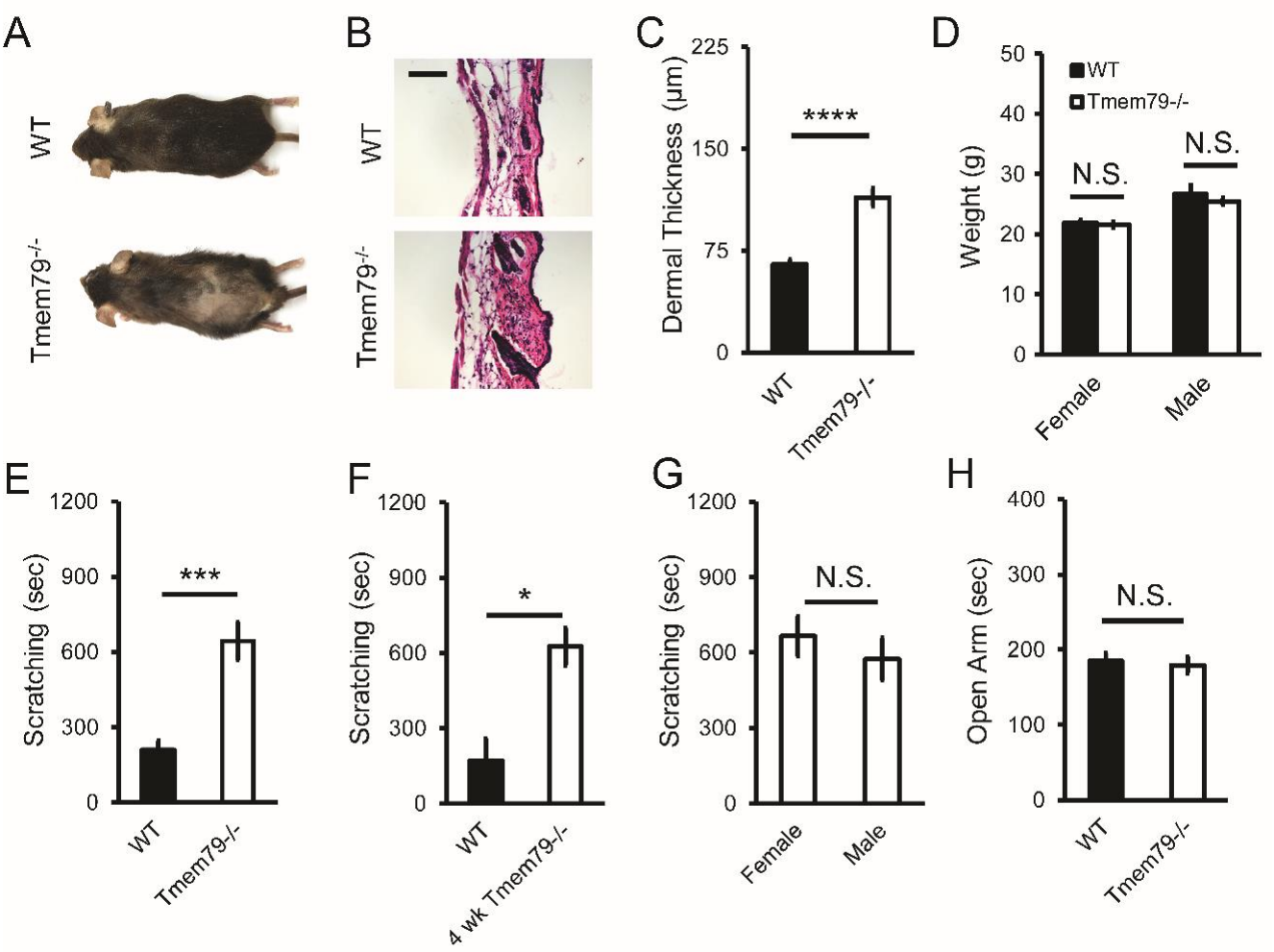

Fig. S1. *Tmem79*$^{-/-}$ mice develop atopic dermatitis (AD) and itch.
(*A*) Representative photographs of pelage of age-matched wild-type (WT, top panel) and *Tmem79*$^{-/-}$ (bottom panel) mice from an overhead vantage. (*B*) Representative micrographs of hematoxylin and eosin stained sections of hairy skin (20 μm) dissected from age-matched wild-type (WT, top panel) and *Tmem79*$^{-/-}$ (bottom panel) mice. Scale bar represents 100 μm. (*C*) Quantification of dermal thickness from dermal sections as represented in (*B*). Data shown are the mean thickness of the dermis of hairy skin sections from age-matched wild-type (WT) and *Tmem79*$^{-/-}$ mice ± s.e.m. (n = 13 sections; ****P<0.0001, Student's t test, two-tailed). (*D*) Quantification of weight of male and female adult wild-type (WT) and *Tmem79*$^{-/-}$ mice. Data shown are the mean weight of mice ± s.e.m. (n = 13 female *Tmem79*$^{-/-}$, 15 female WT, 13 male *Tmem79*$^{-/-}$, 6 male WT; N.S. P>0.05, Student's t test, two-tailed). (*E*) Quantified scratching behavior of adult wild-type (WT) and *Tmem79*$^{-/-}$ mice. Data shown are the mean seconds of scratching from multiple mice of each genotype ± s.e.m. (n = 6 WT, 10 *Tmem79*$^{-/-}$; ***P<0.001, two-tailed). (*F*) Quantified scratching behavior of 4 week old wild-type (WT) and *Tmem79*$^{-/-}$ mice. Data shown are the mean seconds of scratching from multiple mice of each genotype ± s.e.m. (n = 3 WT, 3 *Tmem79*$^{-/-}$; *P<0.05, two-tailed). (*G*) Quantified scratching behavior of adult female and male *Tmem79*$^{-/-}$ mice. Data

shown are the mean seconds of scratching from multiple mice of each genotype ± s.e.m. (*n* = 13 female, 10 male; *P*>0.05, Student's *t* test, two-tailed). (*H*) Elevated plus maze assay of adult wild-type (WT) and *Tmem79*$^{-/-}$ mice. Data shown are the mean seconds multiple mice of each genotype ± s.e.m. occupied the open arm of the plus maze (*n* = 6 WT, 7 *Tmem79*$^{-/-}$; N.S. *P*>0.05, Student's *t* test, two-tailed).

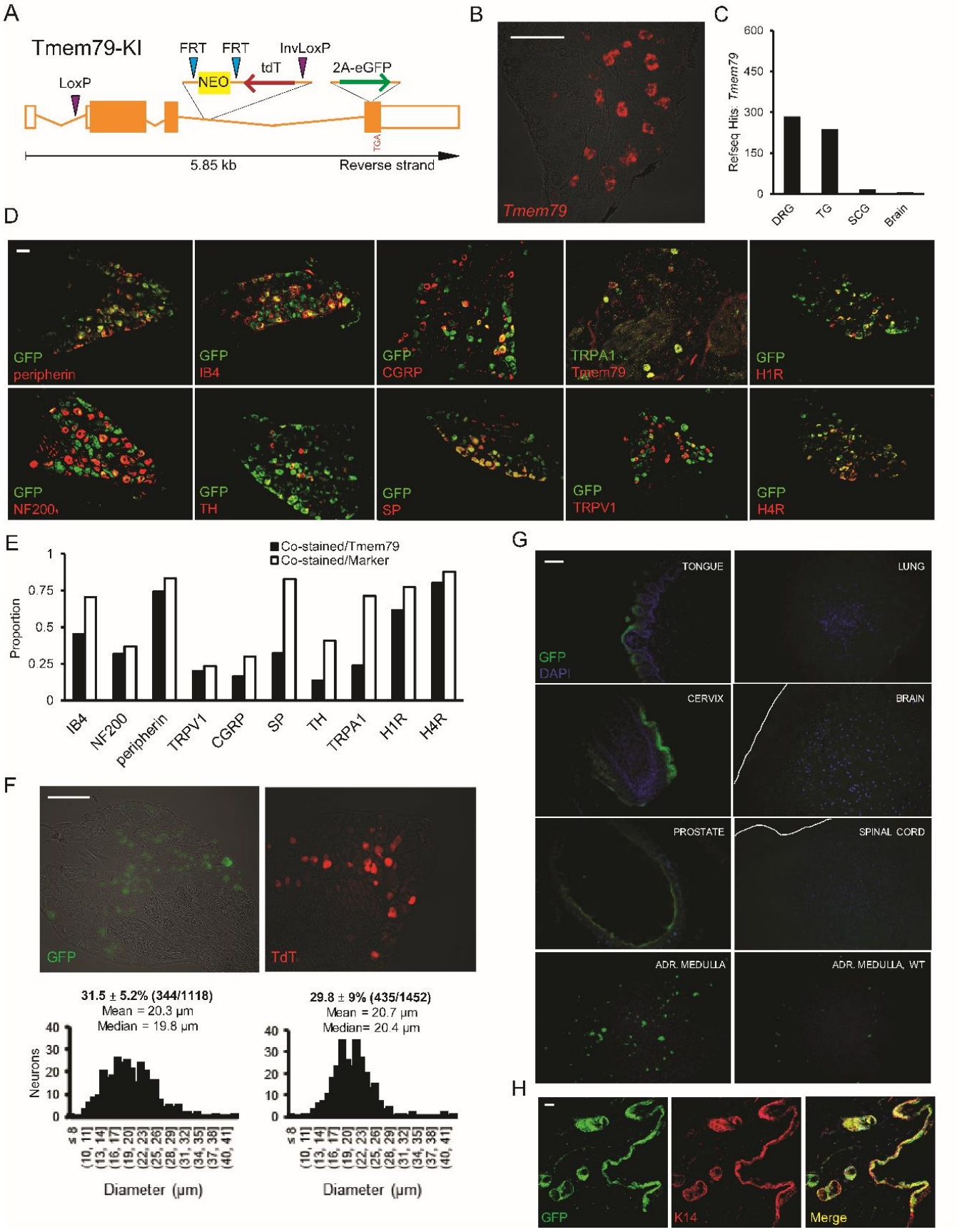
A
Tmem79-KI
FRT
FRT
InvLoxP
tdT
2A-eGFP
NEO
LoxP
TGA
5.85 kb
Reverse strand
B
Tmem79
C
Refseq Hits Tmem79
600
450
300
150
0
DRG
TG
SCG
Brain
D
GFP
peripherin
GFP
IB4
GFP
CGRP
TRPA1
Tmem79
GFP
H1R
GFP
NF200
GFP
TH
GFP
SP
GFP
TRPV1
GFP
H4R
E
Co-stained/Tmem79
Co-stained/Marker
Proportion
1
0.75
0.5
0.25
0
IB4
NF200
peripherin
TRPV1
CGRP
SP
TH
TRPA1
H1R
H4R
F
GFP
TdT
31.5 ± 5.2% (344/1118)
Mean = 20.3 µm
Median = 19.8 µm
29.8 ± 9% (435/1452)
Mean = 20.7 µm
Median= 20.4 µm
Neurons
40
30
20
10
0
≤ 8
(10, 11]
(13, 14]
(16, 17]
(19, 20]
(22, 23]
(25, 26]
(28, 29]
(31, 32]
(34, 35]
(37, 38]
(40, 41]
Diameter (µm)
G
TONGUE
LUNG
GFP
DAPI
CERVIX
BRAIN
PROSTATE
SPINAL CORD
ADR. MEDULLA
ADR. MEDULLA, WT
H
GFP
K14
Merge

Fig. S2. *Tmem79* is expressed in epithelial and nervous tissues.
(*A*) Schematic depicting targeting construct for the generation of the *Tmem79* reporter/conditional knock-in reporter mouse line (*Tmem79*-KI). The construct results in the expression of Tmem79-2A-eGFP under the control of the *Tmem79* promoter. Self-cleavage of Tmem79-2A-eGFP produces separate products TMEM79 and eGFP. Following action of Cre recombinase, TdTomato is knocked in to replace Tmem79-2A-eGFP. (*B*) Representative micrograph of *Tmem79* labeled by fluorescent *in situ* hybridization in dorsal root ganglion (12 µm section). Scale bar represents 100 µm. (*C*) RNAseq hits for *Tmem79* in dorsal root ganglion (DRG), trigeminal ganglion (TG), superior cervical ganglion (SCG), and brain tissue of wild-type mice. (*D*) Representative micrographs of fluorescent co-labeling of dorsal root ganglion sections (12 µm) from adult *Tmem79*-KI mice. Sections stained for immunoreactivity to GFP (green) and binding to IB4, or immunoreactivity to peripherin, CGRP, H1R, NF200, TH, SP, TRPV1, or H4R as indicated (red). *In situ* hybridization co-labeling for *Trpa1* (TRPA1, green) or *Tmem79* (Tmem79, red) also shown. Scale bar represents 50 µm. (*E*) Quantification of co-labeling from micrographs as depicted in (*D*). Co-labeling shown as a proportion of total Tmem79- or marker-positive neurons. Proportions were calculated from counts taken from at least 7 micrographs. (*F*) Representative micrographs of staining for immunoreactivity to GFP (upper left panel, green) or TdT (upper right panel, red) in 12 µm sections of dorsal root ganglion dissected from mice. Images superimposed with brightfield micrographs. Scale bar represents 100 µm. Lower panels provide additional descriptive statistics of GFP- (left) or TdT-positive (right) neurons. Data include proportion of positive neurons/micrograph ± s.e.m. with raw count and population mean and median diameters. *n* = 10 sections (GFP) or 13 sections (TdT) from 3 separate animals. (*G*) Representative micrographs of staining for immunoreactivity to GFP (green) in 20 µm sections of tongue, cervix, prostate, lung, brain, spinal cord, and adrenal medulla (as indicated) dissected from *Tmem79*-KI mice. Nuclei were counterstained with DAPI (blue). Scale bars represent 200 µm. (*H*) Representative micrograph of staining in hairy skin section (20 µm) from *Tmem79*-KI mice for immunoreactivity to GFP (left) or keratin 14 (K14, center). Merged image shown at right. Scale bar represents 10 µm.

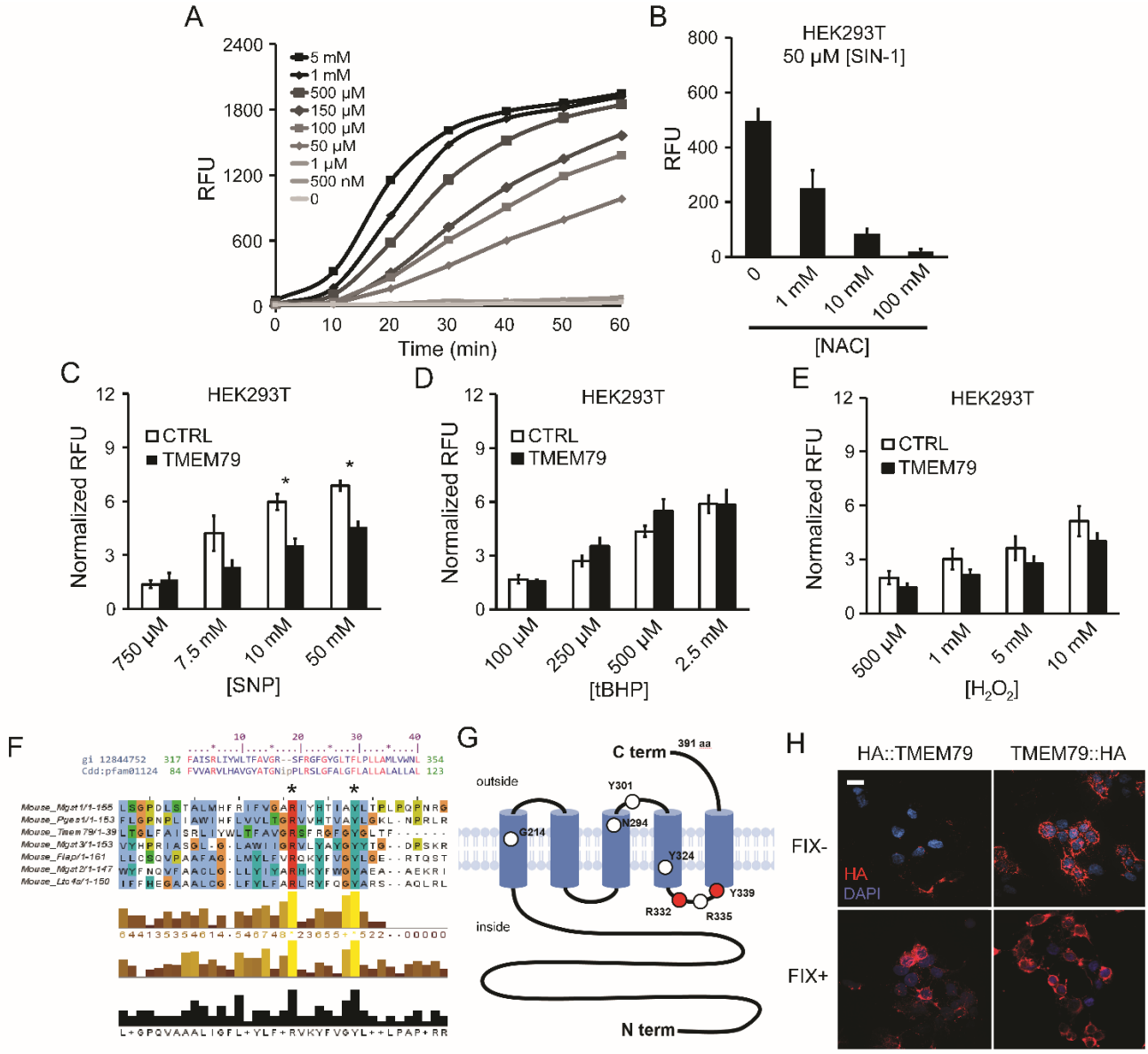

Fig. S3. TMEM79 diminishes reactive oxidative species *in vitro* and has similarity to members of the membrane associated proteins in eicosanoid and glutathione metabolism (MAPEG) superfamily.

(**a-b**) HEK293T cells were transfected with control (CTRL) vector, loaded with DCF dye, then stimulated with SIN-1. (*A*) Quantification of DCF fluorescence in cultures of CTRL HEK293T cells with time in response to various concentrations. DCF fluorescence in HEK293T cells increases in a dose-dependent manner to SIN-1 concentrations with saturation at 5 mM. Data represent mean relative fluorescent units (RFU). *n* = 4 independent experiments with samples run in triplicate. (*B*) Quantification of DCF fluorescence in cultures of HEK293T cells after 30 min incubation with 50 µm SIN-1 and various concentrations of an antioxidant, N-acetylcysteine (NAC). NAC diminishes DCF fluorescence in HEK293T cells in a

dose-dependent manner. Data represent mean RFU ± s.e.m. *n* = 4 independent experiments with samples run in triplicate. (*C-E*) Quantification of DCF fluorescence in cultures of HEK293T cells expressing either control (CTRL) vector or mouse *Tmem79* (TMEM79) following 30 minute incubation with concentrations of oxidants: sodium nitroprusside (SNP), tert-butyl hydroperoxide (tBHP), or hydrogen peroxide (H_2O_2). Data represent mean RFU normalized to baseline ± s.e.m. *n* = 3-4 experiments with samples run in triplicate. **P*< 0.05, Student's *t* test, one-tailed. (*F*) BLAST query and alignment of the primary amino acid sequence of mouse *Tmem79* (top) reveals identity with the MAPEG superfamily. ClustalW2 alignment (bottom) of mouse Tmem79 with mouse MAPEG members *Mgst1*, *Pges1*, *Mgst3*, *Flap*, *Mgst2*, and *Ltc4s*. Asterisk indicates two conserved residues within a region of sequence similarity corresponding to mouse *Tmem79* R332 and Y339. ClustalW2 alignment shown at bottom. (*G*) Mouse *Tmem79* membrane topology as predicted by TMpred with intracellular C terminus (inside). Residues mutated in Fig. 2e are indicated (white and red circles). Conserved residues from ClustalW2 alignment, R332 and Y339, are represented by red circles. (*H*) Representative micrographs of HEK293T stained for immunoreactivity to hemagglutinin (HA, red) without (FIX-, top row) or with (FIX+, bottom row) fixation for permeabilization. HEK293T cells were transfected with vectors for expression of N terminal HA-Tmem79 fusion (HA::TMEM79, left column) or C terminal HA-Tmem79 fusion protein (TMEM79::HA, right column). Scale bar represents 15 µm. Immunostaining in micrographs suggests topology shown in (*G*).

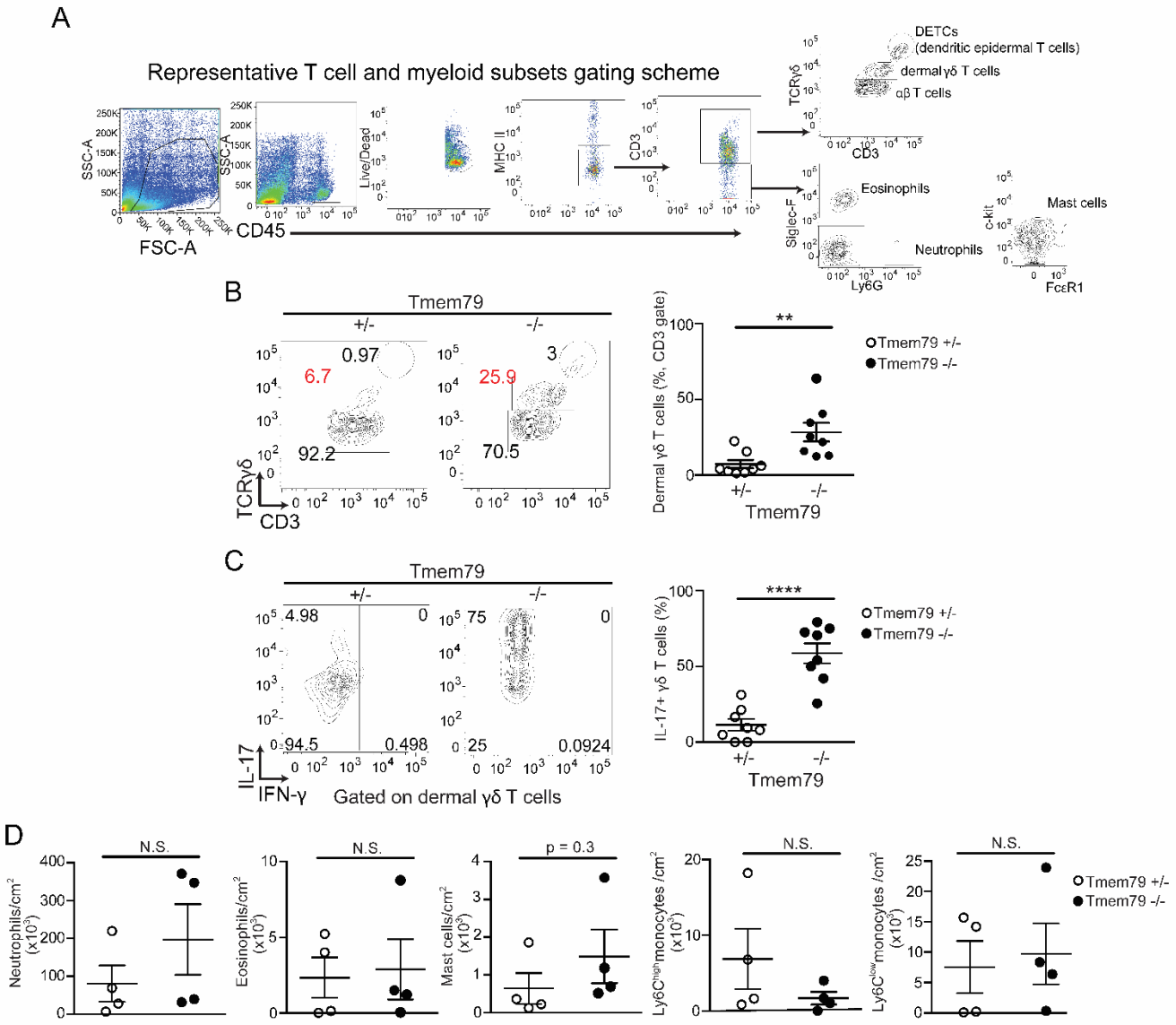

Fig. S4. Preferential accumulation of IL-17-producing dermal γδ T cells in the skin of *Tmem79*$^{-/-}$ mice.

(*A*) Representative gating scheme of immune cell phenotypes in skin by flow cytometry. The gating strategy is shown for neutrophils, eosinophils, mast cells, dendritic epidermal γδ T cells (DETCs), dermal γδ T cells, and αβ T cells. (*B*) Representative flow cytometry plots and percent of dermal γδ T cells in the dorsal skin of *Tmem79*$^{-/-}$ compared to *Tmem79*$^{+/-}$ littermate controls. Plots are pre-gated on live, CD45^{+} CD3^{+} MHC II^{-} cells. Data are mean percentages ± s.e.m. *n* = mice, 8 *Tmem79*$^{+/-}$, 8 *Tmem79*$^{-/-}$ representing two independent pooled sets of 4 mice for each group. ***P*< 0.01, Student's *t* test, one-tailed. (*C*) Representative flow cytometry plots and percent of IL-17^{+} dermal γδ T cells in the skin of *Tmem79*$^{-/-}$ compared to *Tmem79*$^{+/-}$ littermate controls. Plots are pre-gated on dermal γδ T cells (described in *A*). Data are mean percentages ± s.e.m. *n* = mice, 8 *Tmem79*$^{+/-}$, 8 *Tmem79*$^{-/-}$ representing two independent pooled sets of 4 mice for each group.

****P< 0.0001, Student's t test, one-tailed. (D) Absolute number of the indicated immune cells per cm^2 of dorsal hairy skin of *Tmem79*$^{-/-}$ mice compared to *Tmem79*$^{+/-}$ littermate controls. Data are mean number ± s.e.m. n = mice, 4 *Tmem79*$^{+/-}$, 4 *Tmem79*$^{-/-}$ representing two independent pooled sets of 2 mice for each group. N.S. P>0.05, Student's t test, one-tailed.

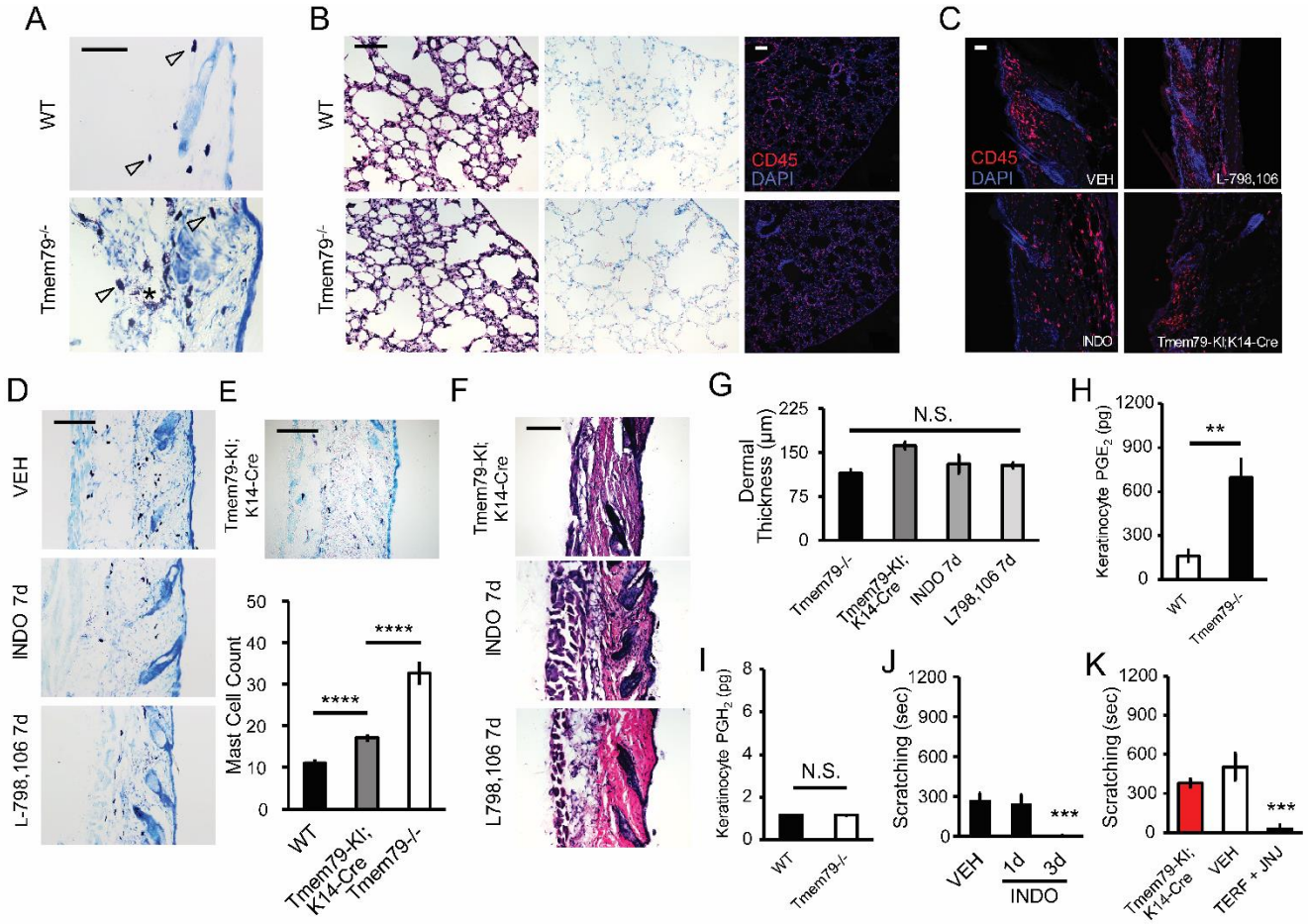

Fig. S5. Interfering with PGE_2-EP3 signaling reverses mast cell accumulation, but not dermal thickness.

(*A*) Representative higher magnification micrographs of toluidine blue O stained hairy skin sections (20 μm) from age-matched wild-type (WT, top panel) or *Tmem79*$^{-/-}$ (bottom) mice. Superficial epidermis is oriented to the right. Hollow arrowheads bring attention to examples of stained mast cells. Asterisk indicates degranulated mast cell(s). Scale bar represents 50 μm. (*B*) Representative micrographs of stained lung sections (20 μm) from age-matched wild-type (WT, top panel) or *Tmem79*$^{-/-}$ (bottom) mice. Staining by hematoxylin and eosin (left column), by toluidine blue O (center column) or for immunoreactivity to CD45 with nuclei counterstained by DAPI (right column). Scale bar represents 100 μm except in right column where it represents 10 μm. (*C*) Representative micrographs of stained hairy skin sections (20 μm) from untreated *Tmem79*-KI;K14-Cre mice or *Tmem79*$^{-/-}$ mice receiving 7 consecutive days of intraperitoneal administration of vehicle (VEH), 10 mg/kg indomethancin (INDO), or 100 mg/kg L-798,106. Superficial epidermis is oriented to the left. Staining for immunoreactivity to CD45 (red) with nuclei counterstained using DAPI (blue). Scale bar represents 10 μm. (*D*) Representative micrographs of toluidine blue O stained hairy skin sections (20 μm) from *Tmem79*$^{-/-}$ mice receiving 7 consecutive days of intraperitoneal administration of vehicle (VEH), 10 mg/kg indomethancin (INDO), or 100 mg/kg L-798,106. Superficial epidermis is oriented to the right. Scale bar represents 100

µm. (*E*) Top panel: Representative micrographs of toluidine blue O stained hairy skin sections (20 µm) from *Tmem79*-KI;K14-Cre. Superficial epidermis is oriented to the right. Scale bar represents 100 µm. Bottom panel: Quantification of mast cells from micrographs represented by top panel and from Fig. 3d. Data shown are the mean mast cell count from fields captured from wild-type (WT), *Tmem79*-KI;K14-Cre, or *Tmem79*$^{-/-}$ mice ± s.e.m. *n* = micrographs, 40 WT, 69 *Tmem79*-KI;K14-Cre, 47 *Tmem79*$^{-/-}$. ****P<0.0001, Holm *t* test, two-tailed. (*F*) Representative micrographs of hematoxylin and eosin stained sections of hairy skin (20 µm) dissected from untreated *Tmem79*-KI;K14-Cre mice or *Tmem79*$^{-/-}$ mice receiving 7 consecutive days of intraperitoneal administration of 10 mg/kg indomethancin (INDO), or 100 mg/kg L-798,106. Scale bar represents 100 µm. (*G*) Quantification of dermal thickness from skin sections as represented in (*F*) and Fig. S1b-c. Data shown are the mean thickness of the dermis in hairy skin sections from mice ± s.e.m. (*n* = 13 *Tmem79*$^{-/-}$, 22 *Tmem79*-KI;K14-Cre, 12 INDO, 24 L-798,106; N.S. P>0.05, Holm *t* test, two-tailed). (*H-I*) ELISA was used to quantify PGE_2 or PGH_2 content from lysed, acutely-dissociated keratinocytes from age-matched wild-type (WT) and *Tmem79*$^{-/-}$. Data represent the average content of PGE_2 or PGH_2 in picograms (pg) from keratinocytes from weight matched skin dissected from separate animals ± s.e.m. (*n* = 3 animals per group; **P<0.01, N.S. P>0.05, Student's *t* test, one-tailed). (*J*) Quantified scratching behavior of adult wild-type mice following 1 or 3 consecutive days of intraperitoneal administration of vehicle (VEH) or 10 mg/kg indomethacin (INDO). Data shown are the mean seconds of scratching from multiple mice in each treatment group ± s.e.m. (*n* = 4; ***P<0.001, Holm *t* test, one-tailed). (*K*) Quantified scratching behavior of adult *Tmem79*-KI;K14-Cre mice at baseline and following intraperitoneal administration of vehicle (VEH) or 20 mg/kg terfenidine+20 mg/kg JNJ-7777120 (TERF+JNJ). Data shown are the mean seconds of scratching from multiple mice in each treatment group ± s.e.m. (*n* = 12 *Tmem79*-KI;K14-Cre, 10 VEH, 7 TERF+JNJ; ***P<0.001, Holm *t* test, one-tailed).

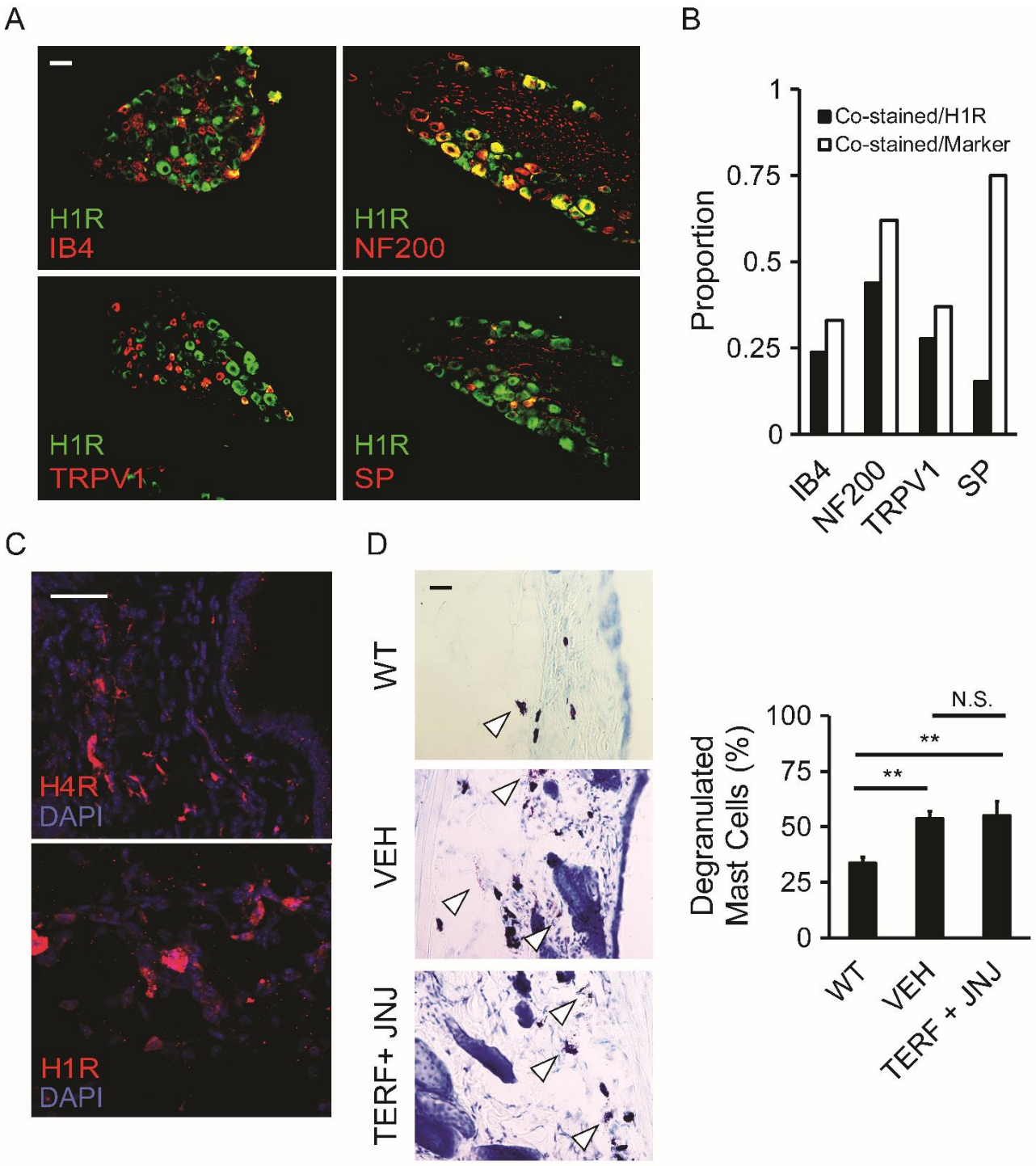

Fig. S6. Blockade of histaminergic signaling does not diminish mast cell degranulation suggesting that neuronal histamine receptors underlie *Tmem79*$^{-/-}$ itch.

(*A*) Representative micrographs of fluorescent co-labeling of dorsal root ganglion sections (12 µm) from adult wild-type mice. Sections stained for immunoreactivity to H1R (green) and binding to IB4, or immunoreactivity to NF200, TRPV1, or SP

as indicated (red). Scale bar represents 50 µm. (*B*) Quantification of co-labeling from micrographs as depicted in (*A*). Co-labeling shown as a proportion of total H1R-positive and marker-positive neurons. Proportions were calculated from counts taken from at least 8 micrographs. (*C*) Representative micrographs of fluorescent co-labeling of hairy skin sections (20 µm) from adult wild-type mice. Sections stained for immunoreactivity to H4R or H1R (red). Nuclei were counterstained with DAPI (blue). Scale bar represents 15 µm. (*D*) Representative micrographs of toluidine blue O stained hairy skin sections (20 µm) from age-matched wild-type (WT, top panel) or *Tmem79*$^{-/-}$ mice 1 hr post intraperitoneal administration of vehicle (middle) or 20 mg/kg terfenidine+20 mg/kg JNJ-7777120 (TERF+JNJ, bottom panel). Superficial epidermis is oriented to the right. Hollow arrowheads bring attention to examples of stained degranulated mast cells. Scale bar represents 100 µm. (*E*) Quantification of mast cells from micrographs represented by (*D*). Data shown are the mean percentage of degranulated mast cells ± s.e.m from fields captured from wild-type (WT) or *Tmem79*$^{-/-}$ mice that received vehicle (VEH) or 20 mg/kg terfenidine+20 mg/kg JNJ-7777120 (TERF+JNJ) treatment (*n* = micrographs, 15 WT, 9 VEH, 9 TERF+JNJ; ***P*<0.01, *****P*<0.0001, One-way ANOVA with Holm-Sidak's multiple comparisons correction).

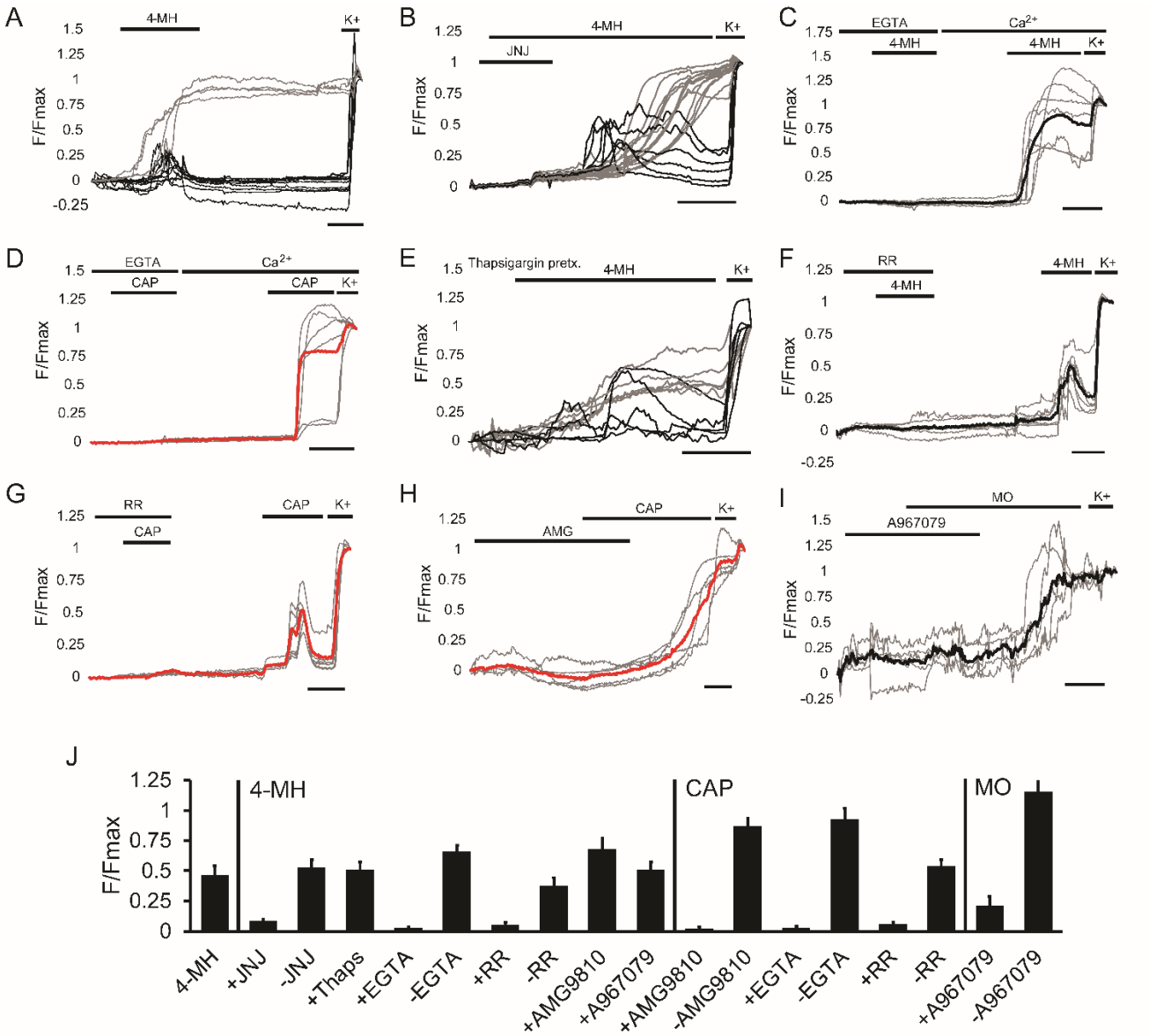

Fig. S7. H4R-agonist triggers TRPV1- and TRPA1-independent calcium entry into sensory neurons.

(*A-I*) Normalized F_{340}/F_{380} calcium imaging traces from adult dorsal root ganglion neurons. Neurons were identified at the conclusion of each experiment by a positive response to elevated extracellular potassium (150 mM KCl, K+). Each trace represents a distinct responder. Scale bars represent 60 sec. (*A-B*) Application of 500 µM 4-methyl histamine (4-MH) produces transient and sustained responses that are blocked by 1 mM JNJ-7777120. (*C-D*) Responses to 500 µM 4-MH and 1 µM capsaicin (CAP) are absent when extracellular calcium is removed (EGTA = Ca^{2+}-free Ringer's solution with 2 mM EGTA). (*E*) Responses to 500 µM 4-MH persist after 90 min pretreatment of neurons with 2 µM thapsigargin. (*F-G*) Responses to 500 µM 4-MH and 1 µM CAP are blocked by 10 µM ruthenium red (RR). (*H-I*) Responses to 1 µM CAP and 1 mM AITC (MO) are blocked by 10 µm AMG9810 (AMG) or 1 mM A967079, respectively. (*J*) Quantification of peak responses from (*A-I*) above. Data shown are mean ± s.e.m.

of peak normalized F_{340}/F_{380} responses (*n* = 13+ responders from 3-4 independent experiments).

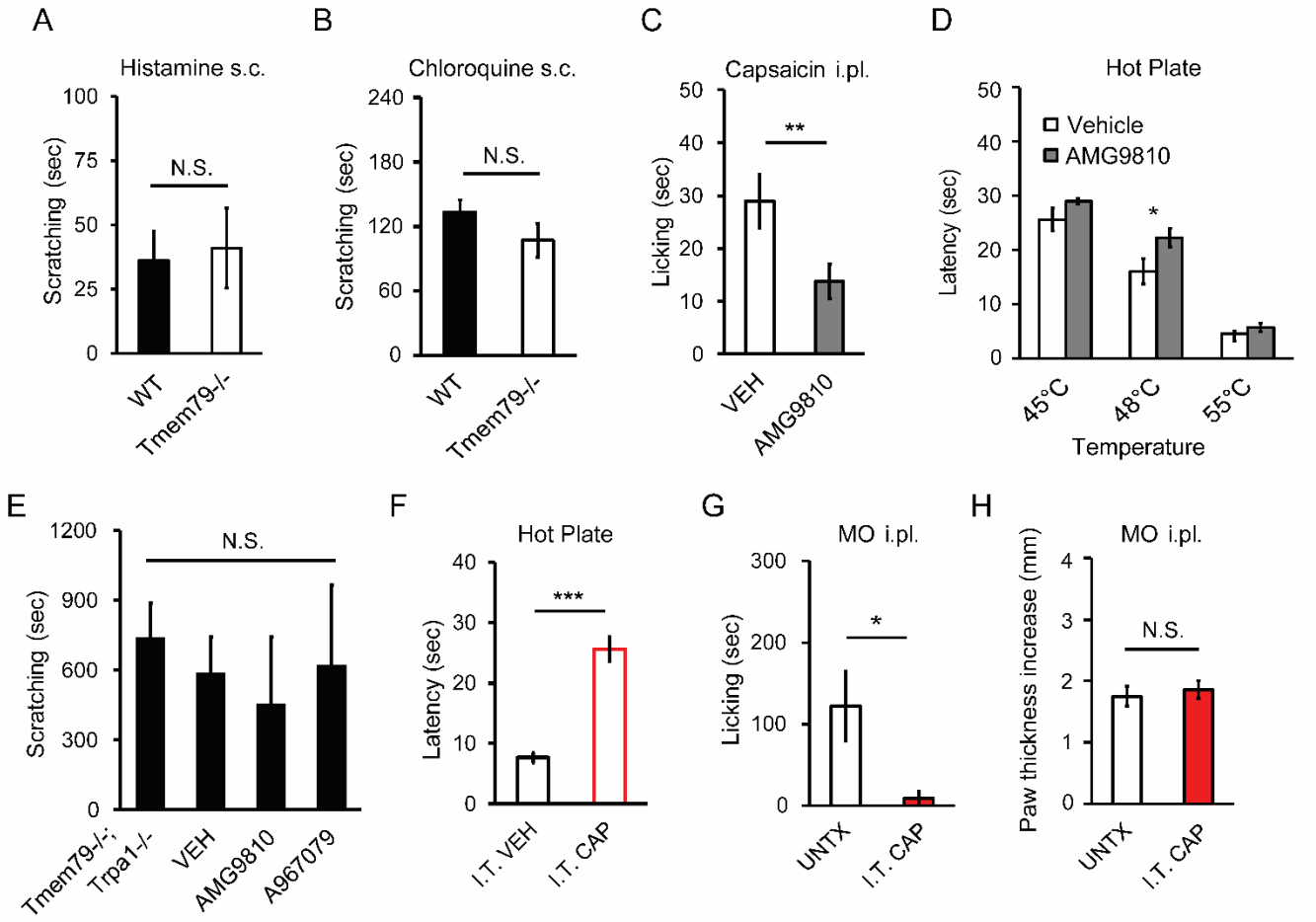

Fig. S8. *Tmem79*$^{-/-}$ histaminergic itch is TRPV1- and TRPA1-independent. (*A*) Quantified scratching behavior of age-matched wild-type (WT) and *Tmem79*$^{-/-}$ mice following subcutaneous administration of histamine (500 µg/100 µL). Data shown are the mean seconds of scratching from multiple mice (*n* = 5 WT, 6 *Tmem79*$^{-/-}$) in each group ± s.e.m. N.S. *P*>0.05, Student's *t* test. (*B*) Quantified scratching behavior of age-matched wild-type (WT) and *Tmem79*$^{-/-}$ mice following subcutaneous administration of chloroquine (200 µg/50 µL). Data shown are the mean seconds of scratching from multiple mice (*n* = 3 WT, 3 *Tmem79*$^{-/-}$) in each group ± s.e.m. N.S. *P*>0.05, Student's *t* test. (*C*) Quantified paw licking of adult *Tmem79*$^{-/-}$ mice in response to 1 µg intraplantar capsaicin following intraperitoneal administration of vehicle (VEH) or 50 mg/kg AMG9810. Data shown are the mean seconds of ipsilateral paw licking from multiple mice (*n* = 8) in each treatment group ± s.e.m. **P*<0.05, Student's *t* test, one-tailed. (*D*) Quantified latency to flinching, licking, or jumping of adult *Tmem79*$^{-/-}$ mice in response to various elevated surface temperatures following intraperitoneal administration of vehicle (VEH) or 50 mg/kg AMG9810. Data shown are the mean seconds to latency of event from 3-5 trials from multiple mice (*n* = 8) in each treatment group ± s.e.m. **P*<0.05, Student's *t* test, one-tailed. (*E*) Quantified scratching behavior of adult *Tmem79*$^{-/-}$;*Trpa1*$^{-/-}$ mice at baseline or following intraperitoneal administration of vehicle (VEH), 30 mg/kg AMG9810, or 50 mg/kg A967079. Data shown are the mean seconds of scratching from

multiple mice (*n* = 4 *Tmem79*$^{-/-}$;*Trpa1*$^{-/-}$ baseline, 7 VEH, 4 AMG9810, 4 A967079) in each treatment group ± s.e.m. N.S. *P*>0.05, Holm *t* test, one-tailed. (*F*) Quantified latency to flinching, licking, or jumping of adult *Tmem79*$^{-/-}$ mice in response to various elevated surface temperatures following intrathecal administration of vehicle (I.T. VEH) or capsaicin (10 µg) (I.T. CAP). Data shown are the mean seconds to latency of event from 3 trials from multiple mice (*n* = 3) in each treatment group ± s.e.m. ***P<0.001, Student's *t* test, one-tailed. (*G*) Quantified paw licking of adult *Tmem79*$^{-/-}$ mice after intrathecal administration of 10 µg capsaicin (I.T. CAP) or wild-type mice (UNTX) in response to 20 µL intraplantar 0.75% mustard oil. Data shown are the mean seconds of ipsilateral paw licking from multiple mice (*n* = 9 UNTX, 7 I.T. CAP) in each treatment group ± s.e.m. *P<0.05, Student's *t* test, one-tailed. (*H*) Quantified paw thickness increase in adult *Tmem79*$^{-/-}$ mice after intrathecal administration of 10 µg capsaicin (I.T. CAP) or wild-type mice (UNTX) in response to 20 µL intraplantar 0.75% mustard oil. Data shown are the mean increase in ipsilateral paw thickness (in mm) from multiple mice in each treatment group ± s.e.m. (*n* = 8 UNTX, 7 I.T. CAP; N.S. *P*>0.05, Student's *t* test, one-tailed).